



Diaphragm air–liquid micro pump applicable to the direct methanol fuel cell



Shi-Min Lee ^{a,*}, Yean-Der Kuan ^b, Min-Feng Sung ^b

^aDepartment of Aerospace Engineering, Tamkang University, 251 Tamsui, Taiwan

^bDepartment of Refrigeration, Air Conditioning and Energy Engineering, National Chin-Yi University of Technology, 411 Taichung, Taiwan

HIGHLIGHTS

- Develop a type of diaphragm air–liquid micro pump to be applied in direct methanol fuel cells.
- The diaphragm air–liquid micro pump can supply both liquid and air at the same pump.
- The developed pump has been successfully demonstrated for applications in pumping the fuel of DMFC.

ARTICLE INFO

Article history:

Received 18 October 2012

Received in revised form

29 January 2013

Accepted 5 March 2013

Available online 25 March 2013

ABSTRACT

This study developed a diaphragm air–liquid micro pump applicable to direct methanol fuel cells. Because direct methanol fuel cells use liquid methanol as fuel and the cathode terminal of the fuel cell uses an active air supply, improving the operational stability of the cell, general fuel cell systems are usually equipped with both liquid and air pumps. The overall consumed power will influence the output power of fuel cells; therefore, the output power can be increased using a pump that supplies both liquid and air.

© 2013 Elsevier B.V. All rights reserved.

Keywords:

Direct methanol fuel cell

Micro pump

Diaphragm

Pneumatic

1. Introduction

Among the numerous types of fuel cells, the proton exchange membrane fuel cell (PEMFC) is commonly used in mobile power systems due to its high efficiency, quiet operation, cleanliness, low operating temperature, and quick startup. Although the PEMFC has a high output power, it requires a perfect air supply system and complicated peripheral control mechanisms [1]. In addition to the advantages of PEMFCs, direct methanol fuel cells (DMFCs) are comprised of a simple system, feature easy fuel refreshment, and operate close to room temperature [2]. Thus, DMFCs are regarded as an alternative power source applicable to 3C (computer, communication, consumer electronics) peripheries.

However, the anode of a DMFC requires a supply of liquid methanol, and the cathode requires an air supply. To maintain

stable and efficient cells [3], active liquid and air pumps are usually used for the operation of fuel cells. At present, there is increasing research interest in micro DMFCs for microminiaturization. This study aims to design and construct a diaphragm air–liquid micro pump. Traditional diaphragm pumps often use electromagnetism or ultrasonication to drive the built-in pump membrane that pushes the liquid. As microelectromechanical technology advances, small, high-efficiency diaphragm pumps are being produced; however, such pumps can convey either liquid or gas but not both at the same time. Other pneumatic pumps are usually used in clean rooms or food production factories requiring cleanliness. However, the microminiaturization of this type of pump is rare. Therefore, this study aims to develop a diaphragm air–liquid micro pump, integrating the advantages of the diaphragm micro pump with the advantages of the pneumatic micro pump to form a diaphragm air/liquid micro pump that transfers the fuel and supplies the cathode terminal with air. Unlike common diaphragm micro pumps, an ultrasonic or electromagnet pump is used as the vibration source for the membrane. The micro pump developed in this study uses a mini DC air pump, and the discontinuous air supply and recoil mechanism embedded in the pump cause the membrane to

* Corresponding author. Department of Aerospace Engineering, Tamkang University, No. 151, Yingzhan Rd., Tamsui Dist., 25137 New Taipei City, Taiwan. Tel.: +886 2 2621 5656x2617; fax: +886 2 2620 9746.

E-mail address: 061503@mail.tku.edu.tw (S.-M. Lee).

oscillate up and down; thus, the combined micro pump can supply both air and fuel.

2. Design and fabrication

2.1. Design concept

To construct the diaphragm air–liquid micro pump, this study first reviewed previous works on diaphragm micro pumps. Nguyen et al. [4] indicated that LIPCA (lightweight piezo-composite actuators) could be used to make a peristaltic pump. Its main operating principle is that three LIPCA pieces are embedded in 0 in the plane array. The liquid-conveying flow channel under the LIPCA is a 50- μm -thick PDMS (polydimethylsiloxane) flow channel created from a SU8 (photoresist), and the volume of the finished micro pump is 20 mm \times 16 mm \times 4 mm. According to experimental results, a 160 V input voltage, 45 mW input power, and 10 Hz incoming frequency resulted in a liquid flow of 900 $\mu\text{L min}^{-1}$. Ma et al. [5] proposed a diaphragm micro pump for use in water-cooling systems. The main operating principle of this pump is that a unidirectional actuator vibrates up and down, causing the compression of a chamber body of a one-way valve to suck liquid from the inlet and compress it towards the outlet. The experimental results revealed that the flow rate was 1.93 mL s^{-1} when the input voltage was ± 50 V. Hsu et al. [6] proposed a diaphragm micro pump using high voltage to deform metal and push liquid peristaltically. The study used silicon wafer, glass, and polymer to construct the micro pump, which is made of polymer. Its advantages include a low cost and better optical transparency, and it is likely to result in a structure with a high depth–width ratio, good biocompatibility, and good mechanical strength. The compression chamber body of this pump applies high pressure to the metal material, resulting in thermal expansion and contraction that deforms the metal and compresses the liquid. Therefore, the study also discussed the influence of common upward and downward deformation modes on the flow rate. The experimental results showed that when the voltage was 100 V and the frequency was 400 Hz, the upward and downward deformations could result in 262.4 $\mu\text{L min}^{-1}$ and 114.8 $\mu\text{L min}^{-1}$ liquid flows, respectively. Trenkle et al. [7] proposed a normally closed peristaltic micro pump for bioengineering applications. The main operating principle of this pump is that three sets of piezoelectric materials are deformed under the input voltage, which deforms the membrane such that it adsorbs liquid and pushes the liquid from the inlet to the outlet, thus conveying the liquid. The experimental results showed that the liquid flow was 120 $\mu\text{L min}^{-1}$ and the backpressure was 40 kPa under the operating conditions of a 140 V (+120 V/–20 V) voltage input and 15 Hz incoming frequency.

Regarding pneumatic micro pumps, Wang et al. [8] developed a pneumatic micro pump for detecting HCV (hepatitis C virus). This pneumatic micro pump uses a series of regular gases to compress the flow channel corresponding to the liquid chamber body and promotes fluid transport. The study used cobweb-like conveying rather than straight-line liquid conveying; thus, various flow channels had coincident flow rates. The compression chamber body of the pump and the micro valve body were made of PDMS to improve air tightness and cleanliness. The experimental results showed that when the incoming frequency was 15 Hz and the air backpressure input was 150 kPa, the liquid flow was 8.4 $\mu\text{L min}^{-1}$. Huang et al. [9] developed a micro vibrator based on the principles of an air drive for producing capsule-like algal cells. The micro pump could be used in bioengineering, but the actuation principle is similar to the micro pump proposed by Wang et al. This micro pump also uses gas to compress the PDMS to cause the sodium alginate inside the flow channel to move. The experimental results

showed that under 10 psi of gas input pressure and an 11 Hz incoming frequency, the liquid flow was 7.98 $\mu\text{L min}^{-1}$. Cheng [10] released a low-energy-consumption methanol fuel distributor and micro methanol fuel-actuated micro pump. This micro pump uses electrolysis to generate bubbles that push the fuel. The fuel output mode is not the common membrane-controlled type; instead, it is controlled by a series of water delivery interfaces and microstructures. A one-inlet four-outlet and a one-inlet three-outlet methanol fuel distributor and micro methanol fuel-actuated micro pump were constructed in the study. The experimental results showed that the one-inlet four-outlet design provided a better flow rate; the liquid flow was 150 nL min^{-1} when the input voltage was 5 V and the incoming frequency was 10 Hz.

Based on the above, this study briefly defines the diaphragm and pneumatic micro pump development technologies: pneumatic micro pumps are usually used for specimens in extra-minute quantities in biomedical engineering and gradually press the liquid pipeline, as do peristaltic pumps, to convey liquid. In other words, the gear for pressing the liquid pipeline of a traditional peristaltic pump is replaced by gas. Regarding the diaphragm micro pump, the liquid is taken in and discharged by the compression of the up-and-down reciprocating vibration of the membrane and the one-way valve mechanism. At present, in this type of micro pump, the most common membrane vibration sources are ultrasonication and electromagnetism. The volume of the ultrasonic type of pump can be as low as 3 mm, with good output flow and pressure. Supplying the cathode terminal of a fuel cell with air improves the stability of the DMFC. Therefore, this study proposes a micro pump that can push liquid as well as recover gas and supply it to the cathode terminal of the fuel cell. It can thus be used as a gas pump as well. This air–liquid pushing pump is an innovative concept. Therefore, this study will develop a diaphragm air/liquid micro pump combining pneumatic and diaphragm micro pumps.

2.2. Diaphragm air/liquid micro pump mechanism design

The diaphragm air/liquid micro pump, as shown in Fig. 1, was designed based on diaphragm [5] and pneumatic [8] micro pumps

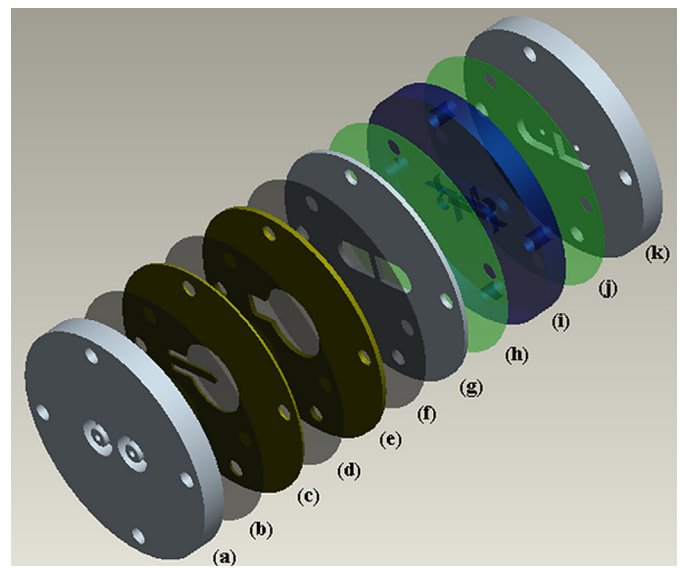


Fig. 1. 3D decomposition chart of the compression chamber body of the diaphragm air/liquid micro pump. (a) PMMA air inlet and outlet plate, (b) PDMS thin film, (c) FR4 recoil mechanism, (d) PDMS thin film, (e) FR4 air compression chamber, (f) PDMS thin film, (g) PMMA liquid compression chamber, (h) PDMS thin film, (i) PMMA one-way valve plate, (j) PDMS thin film, (k) PMMA liquid inlet and outlet plate.

in the literature. This micro pump is comprised of a PMMA (polymethyl methacrylate) air inlet and outlet plate, PDMS thin film, FR4 (fiberglass/epoxy) recoil mechanism, PDMS thin film, FR4 air compression chamber, PDMS thin film, PMMA liquid compression chamber, PDMS thin film, PMMA one-way valve plate, PDMS thin film, and PMMA liquid inlet and outlet plate. Fig. 2 provides the schematic diagram of the air and liquid flow paths of this micro pump, which differ from those of traditional diaphragm micro pumps. The common components of the diaphragm micro pump are shown in Fig. 2(g)–(k), whereas Fig. 2(a)–(f) presents this study's innovative design mechanisms. The common vibration source can be replaced by air. The detailed micro pump operating principle is as described in Section 2.3. The manufacturing process is as shown in Fig. 3. First, the CAD drawings of all pump components were made using computer-aided drawing software. The CAD files were converted using special software into NC machine codes that could be read by CNC and then transferred to the CNC engraving machine to engrave the components. As in the production of the magnetic micro pump, a PDMS membrane was created to compress liquid and provide waterproofing. The production process of this membrane involves mixing the silica gel and hardener into 5 g of PDMS liquid in a ratio of 10:1. Next, the liquid is poured onto the glass center and the rotary coating machine is started, which rotates at 700 rpm for 10 s to complete the PDMS coating. The 4" PDMS-coated glass is placed in a vacuum drying oven, dried at 75 °C for 1 h, and then cut into the required size. When the remaining components have been fabricated by CNC, the cut PDMS membrane and all other components are attached, and the completed compression chamber body of the diaphragm air/liquid micro pump is as shown in Fig. 4.

2.3. Operating principle of diaphragm air/liquid micro pump mechanism

The operating principle of this micro pump is as shown in Fig. 5. If the chamber body is filled with liquid (a), then when air fills the air compression chamber body through the input backboard (b),

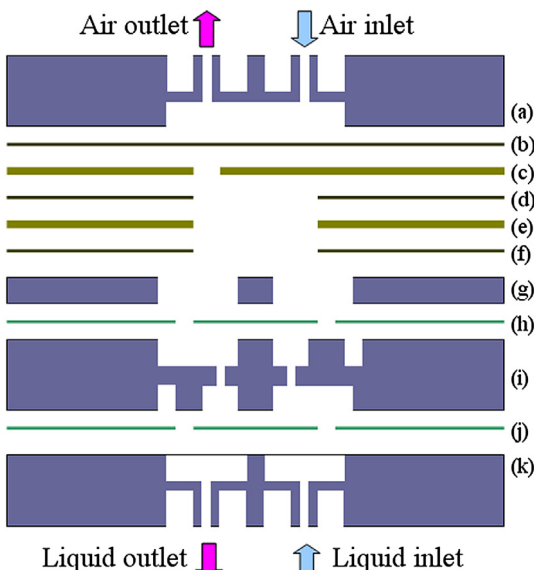


Fig. 2. Plane decomposition chart of the compression chamber body of the diaphragm air/liquid micro pump. (a) PMMA air inlet and outlet plate, (b) PDMS thin film, (c) FR4 recoil mechanism, (d) PDMS thin film, (e) FR4 air compression chamber, (f) PDMS thin film, (g) PMMA liquid compression chamber, (h) PDMS thin film, (i) PMMA one-way valve plate, (j) PDMS thin film, (k) PMMA liquid inlet and outlet plate.

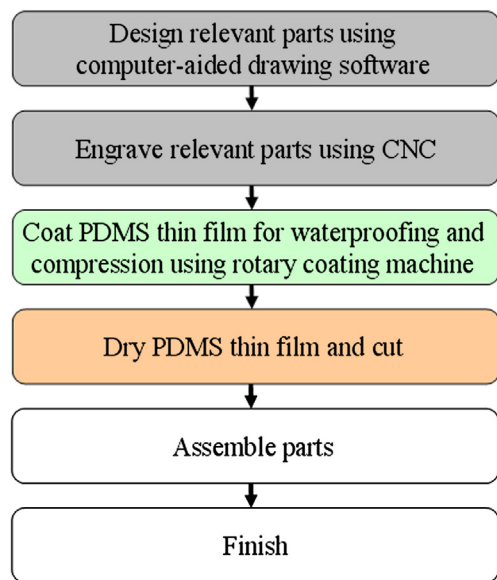


Fig. 3. Production flow of the compression chamber body of the diaphragm air/liquid micro pump.

the membrane under the chamber body is compressed downwards under the pressure of air (c). The liquid in the liquid compression chamber body is then discharged only through the outlet because of the one-way valve (the inlet valve is automatically turned off). When the air supply is stopped, the built-in recoil mechanism of the pump lifts the membrane (d). The liquid is taken in through the inlet as the membrane rises (the outlet valve is automatically turned off), and the liquid flows into the liquid compression chamber body to wait for the next compression. When air refills the air compression chamber body (a), the liquid in the liquid compression chamber body can be recompressed to the outlet (the inlet valve is automatically turned off), and the compression stroke of the pump can be completed by this repeated motion. Therefore, when the inlet air supply frequency is changed, the seesaw frequency for the FR4 plate (see Fig. 2(b)) is also changed, affecting the fluid rate of the pump. The detailed time relationship between the valve on–off and air pump actuation is shown in Fig. 6. Stage 1: the



Fig. 4. Photo of the actual compression chamber body of the diaphragm air/liquid micro pump.

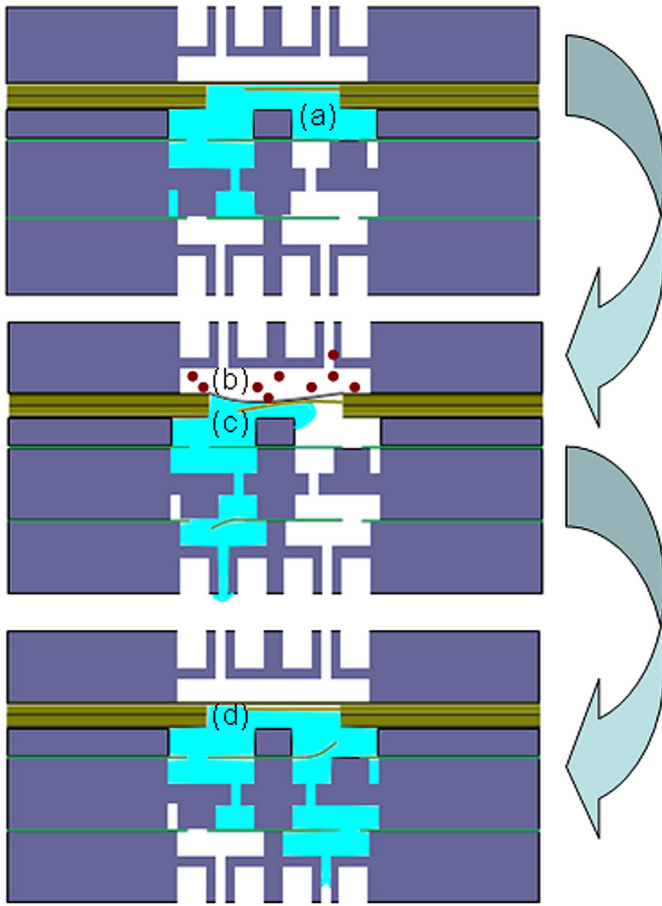


Fig. 5. Schematic of the operation of the compression chamber body of the diaphragm air/liquid micro pump. (a) Chamber body is filled with liquid. (b) Air fills the air compression chamber body through the input backboard. (c) The membrane under the chamber body is compressed downwards under the pressure of air. (d) The built-in recoil mechanism of the pump lifts the membrane.

air pump is started, air fills the air compression chamber body, the outlet valve is turned on, and the liquid in the liquid compression chamber body is discharged. Stage 2: the air pump is shut down; the recoil mechanism inside the pump jacks the membrane up, pushing the liquid into the liquid compression chamber body from the inlet; and then the outlet valve is turned off. When the air is refilled, Stage 1 is re-entered, and the stroke of the micro pump can be completed by repeating this procedure. Thus, the liquid is

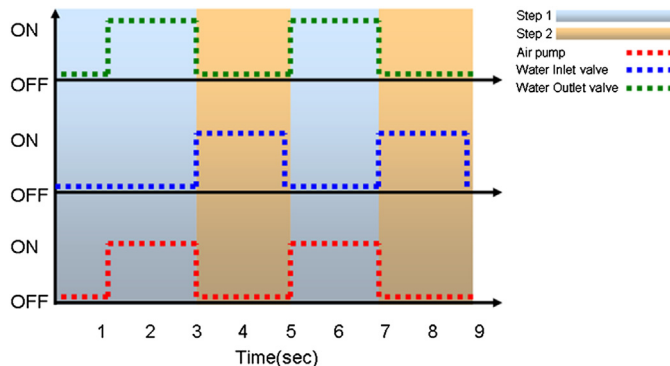


Fig. 6. Valve on–off time in the diaphragm air/liquid micro pump and air pump actuation.

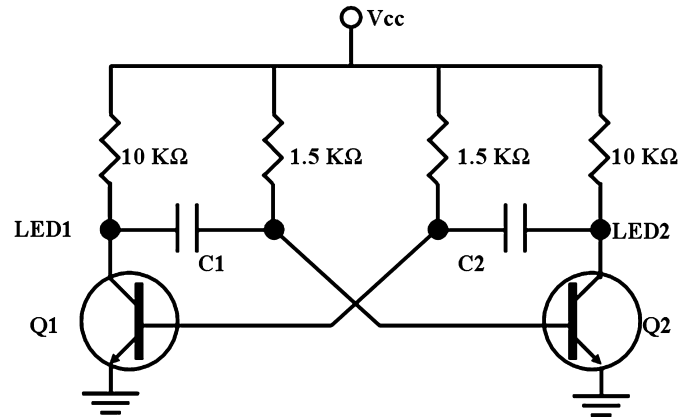


Fig. 7. A stable multivibrator circuit diagram. (a) Resistor, (b) transistor, (c) capacitor, (d) relay, (e) air pump.

conveyed, and the recovered air can be supplied to the cathode terminal of the DMFC. However, discontinuously filled air fills the pump at specific time intervals to effectively push the liquid. Therefore, this study uses a stable multivibrator, as shown in Fig. 7. This circuit is commonly used in various electronic flash units, being a simple, common circuit. The application examples are as shown in the graphics. The basic operating principle of this circuit is that one of two transistors (Q1 and Q2) in the circuit is first powered on when the circuit is supplied with power. If transistor Q1 is powered on first, the C–E terminal of transistor Q1 is powered on, and LED1 lights up. The transistor Q2 then turns into an open circuit, and LED2 goes out. However, capacitor C1 is charged at the same time. When the voltage of capacitor C1 is higher than 0.7 V, the C–E terminal of transistor Q2 is powered on, and LED2 lights up. When the current flows towards Q2, the C–E terminal of transistor Q1 is an open circuit, and LED1 goes out. The current oscillates reciprocally; thus, the current is delivered to the load on the other side without triggering any signal device within the circuit. Therefore, this design is usually used for low-power loads, e.g., LED electronic flash units. According to the preliminary test results, the current delivered to the LED is limited to the transistor; therefore, if the LED power output terminal is directly connected to the mini DC air pump, as adopted in this study, the air pump cannot

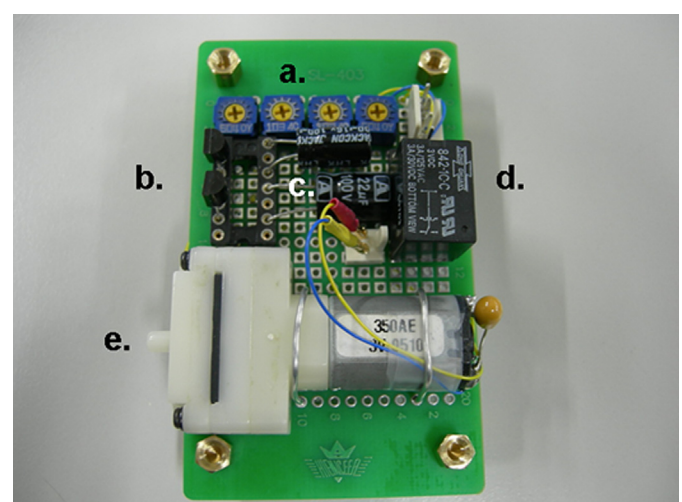


Fig. 8. Actual improved stable multivibrator circuit. (a) Resistor, (b) transistor, (c) capacitor, (d) relay, (e) air pump.

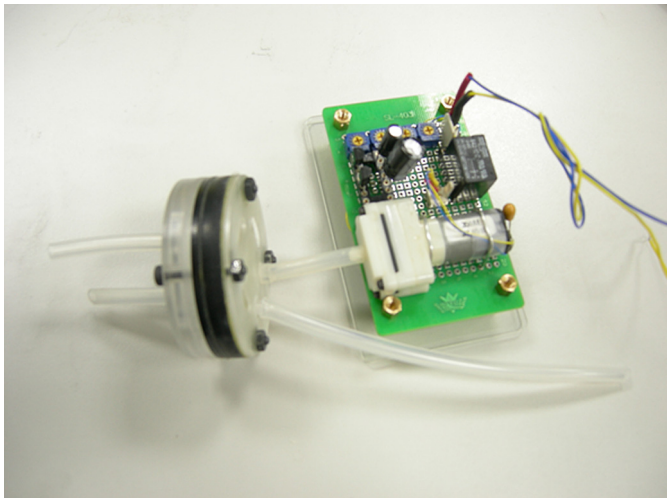


Fig. 9. Actual diaphragm air/liquid micro pump with circuit.

work normally. To solve this problem, this study designed a traditional stable multivibrator as the miniaturized circuit device, as shown in Fig. 8. The main change is that the power output terminal is connected to a 3 V miniature relay. When the voltage signal is delivered to the receiving end of the 3 V relay, the 3 V unlimited to the transistor in the circuit can be delivered to the mini DC air pump. This circuit consists of a resistor, transistor, capacitor, 3 V relay, and mini DC air pump. Finally, the gas supply circuit is connected to the diaphragm pump to complete the diaphragm air/liquid micro pump, as shown in Fig. 9.

3. Experiment construction

The diaphragm air–liquid micro pump designed and produced in this study delivers air intermittently to the air compression chamber body, causing the liquid compression chamber body on the other side to create suction and push out the fluid. Because the gas for this pump is supplied by a 3 V mini DC air pump (0.9 W power consumption), the variable parameter is the frequency of the voltage input, which can be switched by changing the capacitors C1 and C2 in the stable multivibrator circuit. Therefore, this study discussed output combinations at 12 frequencies comprising 100 μ F, 220 μ F, 330 μ F, and 680 μ F. The experimental results showed

Table 1

Time difference resulting from the diaphragm air–liquid micro pump under different capacitance combinations. Units: s.

Power switch	S2: 100 μ F		S2: 220 μ F		S2: 330 μ F		S2: 680 μ F	
	On	Off	On	Off	On	Off	On	Off
S1: 100 μ F	—		1.75	1.25	2.25	1.00	5.75	1.00
S1: 220 μ F	1.25	1.75	—		2.50	2.25	5.50	2.50
S1: 330 μ F	1.25	2.00	2.25	2.75	—		5.75	12.00
S1: 680 μ F	1.50	3.00	2.75	4.75	3.50	5.25	—	

that when two capacitors of the same capacity were inserted in the circuit board because the charging period was too close to the discharge period, the air pump could not be started. Therefore, the combination of identical capacitors was excluded. The experimental structure for discussing the influence of the diaphragm air–liquid micro pump on DMFC performance is shown in Fig. 10; it is composed of a constant-temperature water tank, diaphragm air–liquid micro pump, DMFC cell, data acquisition system, DC electronic loader, and constant-humidity constant-temperature machine. The MEAs adopted in this research were manufactured and assembled by DuPont with a thickness of 1.2 mm. The catalyst load at the anode was 1 mg cm^{-2} Pt/0.5 mg cm^{-2} Ru, and the catalyst load at the cathode side was 1 mg cm^{-2} Pt. The reactive area of the membrane electrolyte assembly (MEA) is 35 mm \times 35 mm.

4. Experiment results

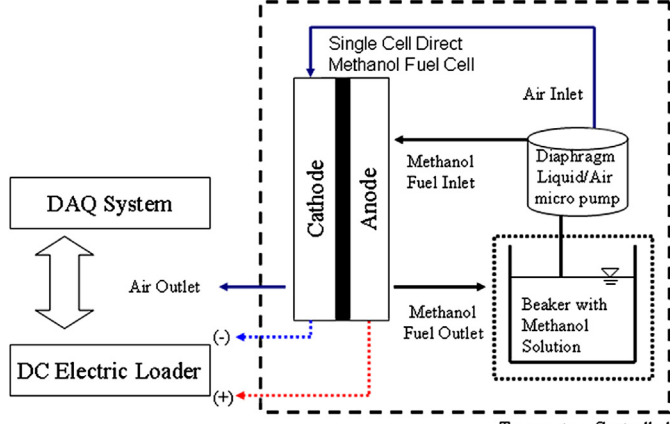
The diaphragm air–liquid micro pump can generate different air supply frequencies by changing the two sets of capacitors, as shown in Fig. 7, to generate 12 time differences, as shown in Table 1. According to the experimental results, when capacitors C1 and C2 are 220 μ F and 100 μ F, respectively, the lowest time difference is generated, in which case the average measured suspension time and air supply time are 1.25 s and 1.75 s, respectively. The maximum time difference occurs when the capacitors C1 and C2 are 330 μ F and 680 μ F, respectively, in which case the average measured suspension time and air supply time are 5.75 s and 12 s, respectively. This time difference between the air supply and suspension will affect the inlet and outlet liquid flow of the pump in a cycle. Table 2 shows the experimental results of the 12 capacitance combinations and conveyable liquid flows. According to the experimental results, the maximum pump flow rate occurs when capacitors C1 and C2 are 100 μ F and 220 μ F, respectively, with an average flow rate of 3.6 cc min^{-1} . The minimum liquid flow occurs when capacitors C1 and C2 are 680 μ F and 220 μ F, respectively, with an average flow rate of 1.5 cc min^{-1} and a gas flow rate of 200 cc min^{-1} . The best performance achieved under optimal DMFC operation conditions is an anode flow rate of 2 cc min^{-1} [3] and a cathode flow rate of 1000 cc min^{-1} [11]. However, the main objective of this study is using a single pump to supply both the fluid and air to achieve lower power consumption. Therefore, this study uses a constant cathode flow rate of 200 cc min^{-1} and an anode flow rate of 3.6 cc min^{-1} . This detail explains the difference in the DMFC performance under the same operation conditions.

Table 2

Flow rate resulting from the diaphragm air–liquid micro pump under different capacitance combinations. Units: cc min^{-1}

	S2: 100 μ F	S2: 220 μ F	S2: 330 μ F	S2: 680 μ F
S1: 100 μ F	—	3.6	3.5	3.4
S1: 220 μ F	3.2	—	3.0	2.6
S1: 330 μ F	2.7	1.5	—	2.3
S1: 680 μ F	1.8	1.5	2.4	—

Fig. 10. Experimental structure using a diaphragm air–liquid micro pump in DMFC.



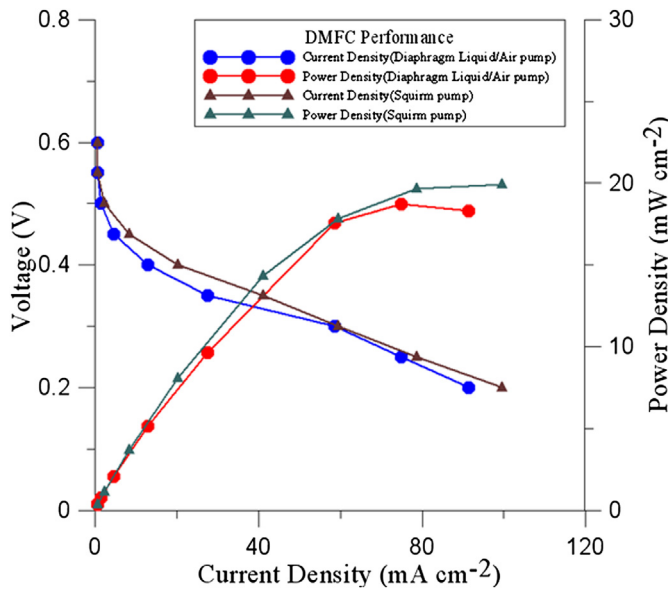


Fig. 11. Experimental results of using a diaphragm air–liquid micro pump in a cell.

Fig. 11 shows the experimental results using a default liquid/air pump and diaphragm air–liquid micro pump in a cell (anode flow rate: 3.6 cc min^{-1} , cathode flow rate: 200 cc min^{-1}). According to the experimental results, when the peristaltic pump is under a 0.2 V load, the current density and power density are 99.54 mA cm^{-2} and 19.91 mW cm^{-2} , respectively. The difference amplitude is also quite small.

5. Conclusions

Based on the experimental results presented above, this study successfully produced a diaphragm air–liquid micro pump that

combines the advantages of diaphragm and air–liquid pumps. This pump delivers liquid and supplies air with an average flow rate of 3.6 cc min^{-1} when the capacitors S1 and S2 are $100 \mu\text{F}$ and $220 \mu\text{F}$, respectively. The minimum liquid flow occurs when the capacitors S1 and S2 are $680 \mu\text{F}$ and $220 \mu\text{F}$, respectively, with an average flow rate is 1.5 cc min^{-1} and a gas flow rate of 200 cc min^{-1} . There is a very small difference between the efficiency of a cell with a diaphragm air–liquid micro pump and that with a peristaltic pump; therefore, this study has successfully produced a diaphragm air–liquid micro pump applicable to direct methanol fuel cells.

Acknowledgements

The authors would like to acknowledge financial support from the National Science Council of Taiwan, R.O.C. (NSC 97-2221-E-167-010 and 98-2221-E-167-024).

References

- [1] J. Larminie, N.S. Sisworahardjo, M.S. Alam, G. Aydinli, *Journal of Power Sources* 177 (2008) 412–418.
- [2] J. Larminie, A. Dicks, *Fuel Cell Systems Explained*, second ed., John Wiley & Sons Ltd., West Sussex, England, 2003.
- [3] Y.-D. Kuan, S.-M. Lee, M.F. Sung, *Renewable Energy* 34 (2009) 1962–1968.
- [4] T.T. Nguyen, M. Pham, N.S. Goo, *Journal of Bionic Engineering* 5 (2008) 135–141.
- [5] H.K. Ma, B.R. Hou, C.Y. Lin, J.J. Gao, *International Communications in Heat and Mass Transfer* 35 (2008) 957–966.
- [6] Y.C. Hsu, J.H. Li, N.B. Le, *Sensors and Actuators A: Physical* 148 (2008) 149–157.
- [7] F. Trenkle, S. Haeberle, R. Zengerle, *Sensors and Actuators B: Chemical* 154 (2011) 137–141.
- [8] C.H. Wang, G.B. Lee, *Biosensors and Bioelectronics* 21 (2005) 419–425.
- [9] S.B. Huang, M.H. Wu, G.B. Lee, *Sensors and Actuators B: Chemical* 147 (2010) 755–764.
- [10] C.M. Cheng, C.H. Liu, *Sensors and Actuators A: Physical* 130–131 (2006) 430–437.
- [11] H. Yang, T.S. Zhao, *Electrochimica Acta* 50 (2005) 3243–3252.